Economic dispatch of power systems with LMP-dependent demands: A non-iterative MILP model☆

Ziqi Shen [a], Wei Wei [a, *], Lei Wu [b], Miadreza Shafie-khah [c], João P.S. Catalão [d]

[a] State Key Laboratory of Power Systems, Department of Electrical Engineering, Tsinghua University, 100084, Beijing, China
[b] ECE Department, Stevens Institute of Technology, 07030, Hoboken, New Jersey, USA
[c] School of Technology and Innovations, University of Vaasa, 65200, Vaasa, Finland
[d] Faculty of Engineering, University of Porto and INESC TEC, 4200-465, Porto, Portugal

ARTICLE INFO

ABSTRACT

The proliferation of demand response programs in the smart grid provides the system operator unique opportunities to reduce the load peak and alleviate network congestions. This paper considers the economic dispatch problem with elastic demands which flexibly respond to the locational marginal prices (LMPs). However, LMP is the dual variable of optimal power flow (OPF) problem and thus is unknown before the OPF problem is solved. Without LMP, the elastic demand is unclear, and the OPF problem cannot be set up. Given this interactive nature, it is difficult to acquire the dispatch strategy as well as the LMP according to the traditional OPF method. This paper thoroughly addresses this problem. Specifically, the limitation of the traditional LMP scheme in the described situation is analyzed. An equilibrium solution may not exist because the demand function and the discontinuous LMP may not have an intersection. To overcome this difficulty, LMP at the discontinuity point is redefined, so that the dispatch problem always has an equilibrium solution. A mixed-integer linear programming model for the economic dispatch problem with LMP-dependent load is proposed, and the equilibrium solution simultaneously offers the dispatch strategy and LMPs. Case studies demonstrate the difficulties of traditional approaches and the effectiveness of the proposed method.

1. Introduction

1.1. Motivation

The increasing demand in modern power systems enlarges the gap between the maximum and minimum load values across a day. Updating power generation and transmission infrastructures is a cost-intensive option and often leads to the less effective utilization of system facilities during off-peak hours. Price-inspired demand response (DR) program encourages consumers to adjust their electricity usage in response to the price signal, and therefore shaves the peak demands, reduces the reserve capacity and alleviates congestion in the power systems [1–3].

DR is a well-studied topic. Typically, DR programs can be roughly divided into direct load control programs and price-incentive programs. In the former category, participators can benefit from subsidy or cost-saving if they allow the operator to directly control their home appliances (such as air conditioners and heaters) in the case of power shortage [4,5]. In the latter category, participants can play a more active role by freely adjusting their electricity usage in response to time-varying electricity prices [6,7]. The study in this paper focuses on the latter category. Several renowned pricing schemes have been proposed and discussed in extensive literature, such as time-of-use pricing, critical peak pricing, and real-time pricing [3]. Since the amount of load reduction is driven by an economic signal rather than controlled directly, to achieve a certain target, it is vital to quantify how consumers would respond to the electricity price.

1.2. Literature review

Modeling DR using various optimization and game models is still an active research field. According to the structure of the optimization problems, existing studies in this direction can be

Nomenclature

Abbreviations

DC	Direct current
DR	Demand response
ED	Economic dispatch
KKT	Karush-Kuhn-Tucker
LMP	Locational marginal price.
LP	Linear program
MILP	Mixed-integer linear program
MINLP	Mixed-integer nonlinear program
OPF	Optimal power flow
SOS2	Special-ordered set of type 2

Parameters

c	Vector of generator cost coefficients
P_D^0	Vector of fixed demands
P_G^L	Vector of generator minimum output
P_G^M	Vector of generator maximum output
F_L	Vector of line flow limits
S	Matrix of power transfer distribution factors

Decision Variables

P_G	Vector of generator output
P_D^R	Vector of elastic demands
ξ	Vector of LMPs
η	Dual variable of power balance condition
π^-, π^+	Dual variables of line flow limit constraints
μ^-, μ^+	Dual variables of generation capacity constraints
λ	Vector of continuous weighting variables
v	Vector of binary variables in SOS2 constraints

roughly classified into three categories.

1) The first category tackles a cost-minimization problem or a profit-maximization problem through a single-level optimization problem under uncertainty and volatility.

For the cost-minimization formulation, DR has been integrated with unit commitment problems [8,9]. Uncertain factors such as renewable generation and system component outage are modeled via scenarios under the stochastic programming framework. In Ref. [8], reserve scheduling is determined to minimize expected total cost. Time-of-use program is designed in Ref. [9] based on an expected reliability index. In the situation that the probability distribution of uncertain factors is not available, robust optimization has been proposed to deal with unit commitment problem considering DR. Robust optimization considers the impact of all possible values of unknown parameters on system performance and copes with the worst case, providing a security guarantee at the cost of a certain level of conservatism, which is applied in Refs. [10,11] to cope with uncertainty from both wind power output and DR mode.

For the profit-maximization problem, the situation is that a price-taker consumer determines the daily usage of electricity while facing uncertain market prices, e,g., the real-time prices in most cases. To avoid financial risks, price uncertainty is taken into account in a stochastic programming model in Ref. [12], robust optimization models in Refs. [13,14], and information gap decision model in Ref. [15]. To reduce the conservatism, a three-stage hybrid stochastic/robust optimization model is suggested in Ref. [16] for strategic bidding of a microgrid in the day-ahead market. In the first two stages, day-ahead prices and renewable output are modeled via scenarios in the stochastic programming framework; in the last stage, uncertainty of real-time market prices is tackled by robust optimization.

Recently, the flexibility potentials of multi-energy systems are exploited in DR programs, where electricity networks' interaction with natural gas system [17,18], combined heat and power systems [19,20], and shared parking station for electric vehicles [21] are

analyzed respectively. A distributionally robust optimization method is proposed in Ref. [22] for gas-electricity system scheduling with DR. Random factors are described by a family of probability distributions whose support set and mean value are given. An interval optimization method is developed in Ref. [23] for gas-electricity system scheduling considering DR and volatile wind power. The work in Ref. [24] utilizes the discrete choice theory and formulates a day-ahead dispatch model for micro-energy system where customers may make energy substitution.

There has also been extensive study on DR integrated with multi-objective dispatch problems where renewable obligation or pollution emission is modeled as extra objective function [25]. A DR mode considering electricity price, consumption hour, and customer type is developed in Ref. [26], and is integrated in Ref. [27] to minimize operational cost and environmental pollution simultaneously via a copula-scenario based uncertainty modeling technique and multi-objective group search optimization. A robust economic dispatch model is developed in Ref. [28] considering DR and renewable obligation with penalty, where energy supply is guaranteed by introducing adequate spinning reserve.

2) The second category addresses simultaneous pricing and DR scheduling in a holistic bi-level optimization problem.

At the retailer level, a retailer arbitrages energy as an intermediary agency between an upstream market and end consumers. Thus, the retailer needs to estimate how consumers would respond to the price and cope with market price uncertainty. In Refs. [29,30], the interaction between the retailer and DR participators are modeled through a bi-level program, while market price uncertainty is taken into account via stochastic programming and robust optimization, respectively. Indeed, when the capacity grows larger, DR has the ability to influence the market price. To model market power of the DR aggregator, the market is cleared subject to the DR bidding strategies. Such clearing mechanisms are formulated by one-leader multi-follower bi-level model in Ref. [31], and stochastic bi-level programming in Refs. [32,33]. To solve such bi-level models, the market-clearing problem in the lower level is

replaced by its Karush-Kuhn-Tucker (KKT) optimality condition and further linearized, and the final problems give rise to mixed-integer linear programs (MILPs). Heat-electricity coupled DR can be formulated using a similar bi-level structure [34]. In Refs. [35,36], multi-period coupling DR is observed in integrated energy systems with electricity, heat, natural gas, and energy storage units under bi-level frameworks. A hybrid pricing method based DR function is expressed using price elasticity in Ref. [37], and the bi-level DR program for the residential microgrid is converted to a single-level mixed-integer nonlinear program (MINLP).

3) The third category endeavors to characterize an equilibrium among multiple DR participants in a competitive market, say, in cases that the market price depends on the total amount of demand.

A supply function bidding based market model is studied in Ref. [38]; a distributed DR algorithm is suggested to achieve the Nash equilibrium, which is shown to maximize social welfare. In Ref. [39], the pricing function is announced by the system operator. A non-cooperative game model is proposed in Ref. [40] to describe the transaction mechanism in the regional energy market considering integrated DR of users. The multi-period DR is considered in Ref. [41] and is also formulated as a Nash equilibrium problem. A Bayesian game among heterogeneous consumers is set forth. Cooperative game theory is employed in Ref. [42] to allocate loss reduction among participators, and in Ref. [43] to retrieve fair pricing among utility companies in the retail market. Evolutionary game is used in Ref. [44] to study the dynamic change of users' preferences.

The problem studied in this paper is a particular sort of DR. It is a variant of the DCOPF for power system economic dispatch, in which elastic loads that flexibly adjust their demand in response to real-time LMPs are taken into account. LMPs are dual variables of power balance constraints and unknown before the optimal solution is found. However, without LMP, the elastic portion of the nodal load is unclear, so the DCOPF problem cannot be set up. Given this interactive nature, it is difficult to acquire the dispatch strategy as well as the LMP according to the traditional OPF method. Such a problem has been studied in Ref. [45] without considering network constraints, so the system shares the same LMP. It is revealed that the uniform pricing market can be unstable with a large fraction of high-sensitive DR loads, and the stability condition is derived using contraction mapping theorem since the model is simple for analytical study. In Ref. [46], the problem is generalized to distribution power market with an alternating current OPF model and distribution LMP. An iterative algorithm is proposed to identify the fixed point of the OPF problem with elastic demands, which interprets the equilibrium of a distribution market. Because LMPs are generally discontinuous, the equilibrium may not exist, and the iterative algorithms may fail to converge.

Methods and modeling assumptions of DR in typical literature mentioned above and in this paper are summarized in Table 1. As is shown in Table 1, the requirement of full DR flexibility,

consideration of network constraints, and existence of market equilibrium have not been fulfilled in a specific model in the previous study. Manipulation of convergence problems and/or network model is quite simplified. It is urged to bridge the gap and produce a realizable optimal dispatch strategy via an optimization model that can guarantee existence of equilibrium.

1.3. Contributions

To address the above challenges, this paper extends the studies in Refs. [45,46] from two aspects, constituting the contributions of this paper:

1) We analyze the market instability caused by the discontinuity of LMP with a complete DCOPF model and network congestion constraints. We proposed to redefine the value of LMP at the discontinuous point of the price curve, so that the existence of an equilibrium solution is guaranteed. In Ref. [45], the instability is caused by slopes of the price curve and the demand curve at the equilibrium point, which is different from that in this paper. Compared with [46], the equilibrium solution always exists by a slight modification on LMP.

2) We propose a non-iterative method to calculate the equilibrium solution which encapsulates the optimal dispatch strategy and LMPs. By concentrating the KKT optimality condition and the linearized demand function, a MILP model is built to compute the equilibrium. We use a dedicated linearization method that incorporates only a few binary variables. Compared with [45,46], there is no convergence issue because iteration is no longer needed. Typical demand functions or inter-period deferring mode are selected in Refs. [28,37] to avoid explicit LMP expression and thus the convergence problem, while in this paper, demand function is submitted by each elastic load, so the flexibility of price-incentive DR can be fully activated.

1.4. Paper organization

The rest of this paper is organized as follows. The dispatch problem and the LMP-dependent load model are introduced in Section 2, followed by the analysis on limitations of traditional LMP scheme and the new definition of LMP at discontinuous points. The equivalent MILP model is developed in Section 3. Case studies are conducted in Section 4. Finally, conclusions are drawn in Section 5.

2. Mathematical model

This paper studies a cost-minimum dispatch problem with LMP-elastic demands, which is executed as follows. First, each elastic load submits a demand function $P_{Dj}^R(\xi_j)$ to the system operator, where ξ_j is the LMP at consumer node j; P_{Dj}^R is the power usage depending on the LMP; Some typical functions covering practical responsive behaviors are suggested in Ref. [45]. Once the system operator has collected demand function bids and traditional inelastic loads, it executes a special OPF procedure, which offers the

Table 1
Review of price-incentive DR modeling methods.

Ref.	Cat.	Research Background of DR	Objective Function	Type of Optimization Problem	Network Model	Consideration of Uncertainty
[9]	1	Time-of-use program in security constrained unit commitment	Expected total generation cost	Stochastic MILP	DC	Yes
[20]	1	Combined heat and power systems	Total cost of energy procurement	Robust optimization and MINLP	None	Yes
[24]	1	Micro-energy system where user can make energy substitution	Real-time net income of micro-energy system	Discrete choice model and MINLP	None	Yes
[25]	1	Microgrid considering DR and internal power market	Minimization of operational cost and microgrid emission	Stochastic linear programming	None	Yes
[28]	1	Multi-objective economic dispatch under renewable obligation	Operating cost minimization, and renewable penetration & user utility maximization	ε-constraint method and MIQP	DC	Yes
[30]	2	Interaction between smart grid retailer and DR participators	Net income of retailer by selling energy to customers	Robust optimization, KKT, and MILP	None	Yes
[33]	2	Short-term scheduling of electricity retailers	Maximization of retailer's expected profit	Two-stage stochastic programming	None	Yes
[37]	2	Day-ahead scheduling of a residential microgrid with DR expressed by price elasticity	Profit maximization	MINLP	AC	No
[39]	3	DR in Smart Grids considering consumer preferences	(generic)	Bayesian game	None	Yes
[42]	3	Loss reduction allocation in smart grid	Loss reduction for maximum DG benefit and load feedback for system stability	Cooperative game	None	Yes
[44]	3	DR Management with multiple utility companies	equilibrium that reduces peak-to-average ratio	Evolutionary game	None	No
[45]	2	General economic dispatch	Operating cost minimization	Iterative convex QP	None	No
[46]	2	Distribution OPF	Operating cost minimization	Iterative SOCP	AC	No
This paper	2	DCOPF	Operating cost minimization	KKT and MILP	DC	No

dispatch strategy and the LMP. We provide additional remarks to clarify the problem.

1) In the proposed method, a consumer can bid a demand function whenever his preference has a change. In practice, this demand function may also resemble a contract or behavior and remains the same in a relatively long period. Therefore, the operator only needs to collect traditional demands, which is the same as in a standard OPF problem.

2) All generators are owned by the system or a non-profit entity, implying that generators possess no strategic behavior or market power. Electricity consumption is paid according to the marginal cost, i.e., the LMP, whose model is well studied. A tutorial can be found in Ref. [47].

3) To set up an OPF, all demands must be given. However, the elastic demand is a function of LMP, the output of OPF. In other words, once the LMP is released, the consumers' electricity usage determined from $P_{Dj}^R(\xi_j)$ must be equal to the demand used in the OPF problem. In this regard, the dispatch problem in this paper cannot be directly solved in the same way as the traditional OPF.

2.1. DCOPF with LMP-elastic demands

The problem is formally stated as follows:

$$\min \quad c^T P_G \tag{1a}$$

$$\text{s.t. } \mathbf{1}^T P_G - \mathbf{1}^T P_D = 0 : \lambda \tag{1b}$$

$$-F_L \leq S(A P_G - B P_D) \leq F_L : \pi^-, \pi^+ \tag{1c}$$

$$P_G^L \leq P_G \leq P_G^M : \mu^-, \mu^+ \tag{1d}$$

together with

$$P_{Dj} = P_{Dj}^0 + P_{Dj}^R(\xi_j), \quad \forall j \tag{1e}$$

$$\xi = \lambda \cdot \mathbf{1} - S^T(\pi^+ - \pi^-) \tag{1f}$$

In problem (1), matrix A/B in (1c) reconciles the dimensions between vector P_G/P_D and matrix S; Greek letters following a colon represents the dual variables; $\mathbf{1}$ is an all-one vector with the same dimension as c. Objective (1a) minimizes the generation cost; (1b)-(1d) are system-wide power balance, line flow limits, and generator capacity constraints, respectively. In contrast to a traditional OPF problem, the nodal demand vector P_D consists of a fixed part P_D^0 and a LMP-elastic part P_D^R as in (1e), and the LMP ξ intrinsically depends on the dual variables in accordance with (1f), so does P_D.

2.2. Analysis of the limitation of traditional LMP

A fixed-point method to solve problem (1) is outlined in Algorithm 1 (Alg-FP for short). However, a fixed point may not

exist, because LMP is generally discontinuous [48]. In such cir-
cumstances, Alg-FP may fail to converge. This phenomenon is
analyzed as follows.

Algorithm 1
Alg-FP

Step 1: Choose an initial value of system demand.
Step 2: Solve DCOPF problem (1a)-(1d) with given demands.
Step 3: Retrieve dual variables, update LMP and elastic demands according to
(1f) and (1e), respectively.
Step 4: If the change of elastic demands in two successive iterations is smaller
than a certain threshold, terminate; otherwise, return to Step 2.

Consider a simple system with three buses and two lines illus-
trated in Fig. 1. Parameters of components are given in the figure.
Now we consider the LMP as a function of demand at load bus D. If
$d \leq 150$ MW, the demand is served by unit G_1, so the LMP is equal to
the marginal cost $c_1 < c_2$. If $d > 150$ MW, the incremental demand is
served by unit G_2, so the LMP is qual to c_2. The LMP curve is plotted
in Fig. 2(a). It is discontinuous at $d = 150$ MW. When the demand is
inelastic, the demand function and the LMP curve intersect at the
red point in Fig. 2(a).

When DR is taken into account, the situation is different. The
simplest DR curve is depicted in Fig. 2(b): when LMP is either too
high or too low, the demand is a constant; otherwise, the demand is
a linear function in LMP. In particular, the DR function and the LMP
curve may not have an intersection. In such a circumstance, Alg-FP
will not converge, as illustrated in Fig. 2(b). Suppose the initial
point is I, the iterations repeat with a period of 2. Such kind of
instability is not caused by the choice of initial point; instead, it is
the consequence of the way how LMPs are defined. To overcome
this issue, we need to analyze and redefine the values of LMP at
discontinuous points.

2.3. Definition of LMP at discontinuous points

To obtain deeper insights of the above example, we write out the
KKT condition at the discontinuous point

$$c_i = \lambda - \mu_i^+ + \mu_i^- - \pi_i^+ + \pi_i^-, \ i = 1, 2 \tag{2a}$$

$$0 \leq \pi_i^+ \perp f_{im} - p_{gi} \geq 0, \ 0 \leq \pi_i^- \perp p_{gi} \geq 0, \ i = 1, 2 \tag{2b}$$

$$0 \leq \mu_i^+ \perp p_{im} - p_{gi} \geq 0, \ 0 \leq \mu_i^- \perp p_{gi} \geq 0, \ i = 1, 2 \tag{2c}$$

$$p_{g1} + p_{g2} = d \tag{2d}$$

where notation $0 \leq a \perp b \geq 0$ stands for complementarity and
slackness conditions $a \geq 0$, $b \geq 0$, $a^T b = 0$. Since both of a and b are
non-negative vectors, $a^T b = 0$ implies $a_i b_i = 0$, $\forall i$ elementwise.
According to the parameters given in Fig. 1, at the point where LMP
is discontinuous, generation lower and upper bounds in (2c) for
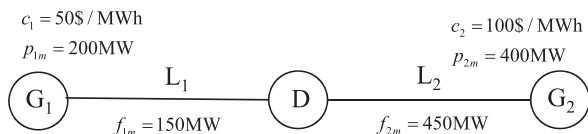unit G_1 are inactive, and thus $\mu_1^+ = \mu_1^- = 0$; generation upper

bound in (2c) for unit G_2 is inactive, so $\mu_2^+ = 0$; transmission upper
bound in (2b) for line L_1 (L_2) is active (inactive), implying $p_{g1} = f_{1m}$,
$\pi_1^+ \geq 0$, $\pi_2^+ = 0$; transmission lower bound in (2b) for line L_1 (L_2) is
inactive (active), indicating $\pi_1^- = 0$, $\pi_2^- \geq 0$.

According to above analysis, at the discontinuous point, the KKT
conditions become

$$c_1 = \lambda - \pi_1^+, \ c_2 = \lambda + \mu_2^- + \pi_2^- \tag{3a}$$

$$f_{1m} = d(\lambda - \pi_1^+ + \pi_2^-) \tag{3b}$$

where $d(\cdot)$ and $\lambda - \pi_1^+ + \pi_2^-$ represent the demand function and
LMP at bus D, respectively.

If $d(\cdot)$ is a constant, equation set (3) is underdetermined; the
KKT condition (2) has infinitely many feasible solutions, for
example, $\lambda = c_1$, $\pi_1^+ = \mu_2^- = \pi_2^- = 0$ together with those already
determined satisfy KKT condition (2), and the corresponding LMP is
$\xi^* = \lambda - \pi_1^+ + \pi_2^- = c_1$. In fact, by choosing different values of dual
variables, the LMP can take any value in the interval $[c_1, c_2]$, and ξ^* is
the minimum price that consumers prefer to pay. Therefore, the red
point in Fig. 2(a) is adopted in practice.

Taking DR into consideration, $d(\cdot)$ is a function in the LMP which
is equal to $\lambda - \pi_1^+ + \pi_2^-$. Since μ_2^- does not impact LMP, we simply set
it to 0; then equation set (3) is properly defined. It includes three
equations in variables λ, π_1^+, and π_2^-, and thus can be solved to
derive a unique solution. From Fig. 2(b) we can see that equation set
(3) has a unique solution marked by a red point.

If the demand function and the LMP curve intersect at the flat
region, such as in Fig. 3(a), we can observe that the demand is
locally non-elastic, so the situation can be treated as the traditional
OPF, as long as the flat region where the intersection point rests in
can be determined in advance. In Fig. 3(b), although the demand is
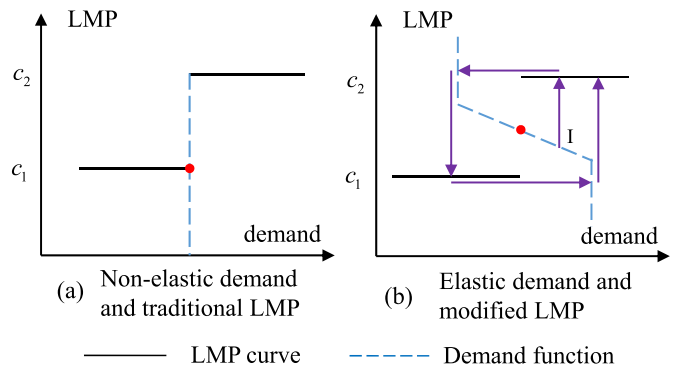elastic, the traditional Alg-FP method can still converge.

Fig. 2. Definition of LMP at the discontinuous point.

c₁ = 50$ / MWh
$p_{1m} = 200$MW

c₂ = 100$ / MWh
$p_{2m} = 400$MW

$f_{1m} = 150$MW $f_{2m} = 450$MW

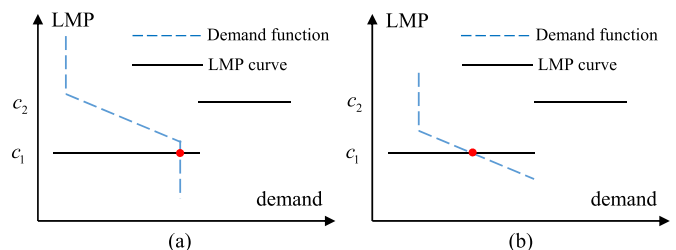**Fig. 1.** A two-node system for the illustration of market instability.

Fig. 3. Flat intersections do not cause instability.

According to above discussions, to dispatch a power system with LMP-dependent demands, we have to define the value of LMP at discontinuous points properly. Inspired by the example, we give the following descriptive definition:

At discontinuous points, the LMP is determined by a set of equations comprised of KKT conditions and demand functions.

Based on this definition, the properties of the optimal solution are discussed as follows.

Existence. As LMP can take any value in $[c_1, c_2]$ in the new definition, the LMP curve can be regarded as continuous. Furthermore, the demand function is also continuous, the two curves must have an intersection since the demand becomes inelastic when the price is either too high or too low.

Uniqueness. In practice, elastic demands decrease with the increase in price. If the LMP curve is increasing in demand, the intersection is also unique. However, in a large-scale system, the LMP depends on all nodal demands, and the situation can be very complicated. A counter-intuitive example can be found in Ref. [47]. Nonetheless, for a real power system, it is acceptable to assume that LMP curve is increasing in demand.

3. An equivalent MILP model

A monolithic MILP model will be developed in this section to solve problem (1) without iteration.

3.1. KKT condition of the OPF problem

To solve problem (1b)-(1d) while considering the response (1e)-(1f) of elastic demands, we need to optimize primal and dual variables at the same time. To this end, we write out the following KKT condition of problem (1b)-(1d) while treating P_D as constant

$$c + \lambda \cdot \mathbf{1} + A^T S^T (\pi^+ - \pi^-) + \mu^+ - \mu^- = 0$$
$$0 \leq \pi^- \perp S(AP_G - BP_D) + F_L \geq 0$$
$$0 \leq \pi^+ \perp F_L - S(AP_G - BP_D) \geq 0 \qquad (4)$$
$$0 \leq \mu^- \perp P_G - P_G^L \geq 0, \ 0 \leq \mu^+ \perp P_G^M - P_G \geq 0$$
$$\mathbf{1}^T P_G - \mathbf{1}^T P_D = 0$$

Dual variables are explicitly modeled in KKT condition (4). We can solve (4) with (1e)-(1f) simultaneously, giving rise to a nonlinear complementarity problem. However, two difficulties prevent such a complementarity problem from being solved efficiently. One is the nonlinearity of the demand function $P_{Dj}^R(\xi_j)$ in (1e); the other is the complementarity constraints themselves, because they violate constraint quantification conditions at any feasible point [49] and cause numeric issues.

To circumvent these difficulties, we endeavor to develop a monolithic MILP model, which has the same optimal solution as problem (1), as MILPs can be reliably solved by commercial software. On this account, we have to reformulate the demand function and the complementarity constraints in forms that are compatible with MILP solvers.

3.2. Linearizing the demand function

We express the nonlinear demand function $P_{Dj}^R(LMP_j)$ via a piecewise linear (PWL) function with 0−1 variables. Suppose we have a collection of samples (p_{dj}^{rk}, ξ_j^k), $k = 0, 1, \cdots, K$, where $p_{dj}^{rk} = P_{Dj}^R(\xi_j^k)$. Associating each pair (p_{dj}^{rk}, ξ_j^k) with a non-negative weight coefficient γ_j^k, the PWL demand function is given by

$$\xi_j = \sum_k \gamma_j^k \xi_j^k, \ P_{Dj}^R = \sum_k \gamma_j^k p_{dj}^{rk}, \ \forall j \qquad (5)$$

$$(\gamma_j^0, \cdots, \gamma_j^K) \in \Delta_{K+1} \text{ is SOS2}, \ \forall j \qquad (6)$$

where $\Delta_{K+1} = \{x \in \mathbb{R}^{K+1} | x \geq 0, \mathbf{1}^T x = 1\}$ stands for a probability simplex. In a special-ordered set of type 2 (SOS2), at most two adjacent elements can take strictly positive values while remaining ones are 0. Using the technique in Ref. [50], SOS2 constraint can be formulated as MILP form with $\lceil \log_2 K \rceil$ 0−1 variables. Specifically, we use PWL function with $K = 8$. In such a circumstance, the SOS2 constraint in (6) evolves

$$\left\{ \begin{array}{l} \gamma_j^0 + \gamma_j^1 + \gamma_j^2 + \gamma_j^3 \leq 1 - \nu_{1j} \\ \gamma_j^5 + \gamma_j^6 + \gamma_j^7 + \gamma_j^8 \leq \nu_{1j} \\ \gamma_j^0 + \gamma_j^1 + \gamma_j^6 \leq 1 - \nu_{2j} \\ \gamma_j^3 + \gamma_j^4 + \gamma_j^8 \leq \nu_{2j} \\ \gamma_j^0 + \gamma_j^4 + \gamma_j^5 \leq 1 - \nu_{3j} \\ \gamma_j^2 + \gamma_j^7 + \gamma_j^8 \leq \nu_{2j} \\ \nu_{1j}, \nu_{2j}, \nu_{3j} \in \{0, 1\} \end{array} \right\}, \ \forall j \qquad (7)$$

In (7), only three binary variables ν_{1j}, ν_{2j}, ν_{3j} are introduced to linearize one demand function. Suppose the demand function $P_{Dj}^R(\xi_j)$ is second-order continuously differentiable on interval $[\xi, \xi + h]$, and its linear interpolation function is denoted by $P_{1j}(\xi_j)$. Let D_M denote the upper bound of the second-order derivative of P_{Dj}^R. It can be proved that the error bound satisfies

$$\left| P_{Dj}^R(\xi_j) - P_{1j}(\xi_j) \right| \leq \frac{D_M h^2}{8} = O\left(h^2\right) \qquad (8)$$

When we perform piecewise linear interpolation on $P_{Dj}^R(\xi_j)$ in interval $[\xi^0, \xi^m]$ with even sampling distances, the maximum error of approximation is $O([(\xi^m - \xi^0)/K]^2)$, which means that the error can be arbitrarily small by adding more sampling points. Furthermore, the SOS2 constraint incorporates only $\lceil \log_2 K \rceil$ 0−1 variables. Therefore, the piecewise linear function can provide a satisfactory approximation of the nonlinear demand function when a larger K is

chosen. The proof of error bound (8) is given in Appendix A.

3.3. The MILP model

To explain the method more clearly without trapped into extensive symbols and notations, the complementarity constraints are denoted as $0 \leq a \perp b \geq 0$, where b includes all dual variables, and each element of a is a linear function depending on P_G. The most renowned method for linearizing complementarity constraints is the Fortuny-Amat approach in Ref. [51], leading to

$$0 \leq a \leq M(\mathbf{1} - z), \ 0 \leq b \leq Mz \qquad (9)$$

where z is a vector that consists of 0−1 variables with a compatible dimension; M is a large enough constant. The binary value of z_i imposes either a_i or b_i being at 0, and thus complementarity conditions in (4) hold. However, with this technique, the MILP model does not have an objective function, and the branch-and-bound procedure lacks sufficient information to prune unnecessary branches.

Alternatively, we try to minimize $a^T z + b^T(\mathbf{1} - z)$ subject to $a \geq 0$, $b \geq 0$ and other constraints. If a feasible solution satisfying complementarity exists, the optimal value must be 0. The situation is a little different. In (9), $z_i = 0$ implies $a_i = 0$, while in the above objective function, $z_i = 1$ implies $a_i = 0$. The objective function is nonlinear as it contains bilinear terms like $z_i a_i$ and $z_i b_i$. These bilinear terms comprised of a binary variable and a continuous variable can be equivalently converted into an MILP compatible form with an auxiliary continuous variable w_i satisfying

$$0 \leq w_i \leq Mz_i, \ 0 \leq a_i - w_i \leq M(1 - z_i) \qquad (10)$$

For problem (4), we seek to minimize

$$
\begin{aligned}
\text{Obj} = &(\mathbf{1} - z_1)^T \pi^- + z_1^T (f + F_L) \\
&+ (\mathbf{1} - z_2)^T \pi^+ + z_2^T (F_L - f) \\
&+ (\mathbf{1} - z_3)^T \mu^- + z_3^T \left(P_G - P_G^L \right) \\
&+ (\mathbf{1} - z_4)^T \mu^+ + z_4^T \left(P_G^M - P_G \right)
\end{aligned} \qquad (11)
$$

where $f = S(AP_G - BP_D)$ is the line power flow vector.

Let Obj-Lin be the linear objective function after performing linearization technique in (10) to (11), and Cons-Lin the additional constraints in the form of (10) which are introduced by the linearization procedure. The proposed MILP model for problem (1) is cast as

$$
\begin{aligned}
\min \quad & \text{Obj} - \text{Lin} \\
\text{s.t.} \quad & \text{Cons} - \text{Lin} \\
& c + \lambda \cdot \mathbf{1} + A^T S^T (\pi^+ - \pi^-) + \mu^+ - \mu^- = 0 \\
& \mathbf{1}^T P_G - \mathbf{1}^T P_D = 0, \ f = S(AP_G - BP_D) \\
& \pi^- \geq 0, \ \pi^+ \geq 0, \ -F_L \leq f \leq F_L \\
& \mu^- \geq 0, \ \mu^+ \geq 0, \ P_G^L \leq P_G \leq P_G^M \\
& \lambda - S_j^T (\pi^+ - \pi^-) = \sum_{k=0}^{8} \gamma_j^k \xi_j^k, \ \forall j \\
& P_{Dj} = P_{Dj}^0 + \sum_{k=0}^{8} \gamma_j^k p_{dj}^{rk}, \ \forall j \\
& \left(\gamma_j^0, ..., \gamma_j^8 \right) \in \Delta_9, \ \forall j \\
& \text{SOS2 constraint (7)}, \ \forall j
\end{aligned} \qquad (12)
$$

where S_j is the j-th column of matrix S. A few more discussions are provided below.

1) The selection of variable bounds. The proper value of M depends on the bounds of primal and dual variables. Because dual variable can be interpreted as the incremental cost at optimum with respect to per unit change in constraint right-hand coefficient, the bounds of μ_i^- and μ_i^+ can be chosen by multiplying the generator marginal cost c_i with a scalar $\sigma > 1$. The bounds of λ can be set as $\sigma \max_i \{c_i\}$. A rough estimation of π^- and π^+ can be obtained from sensitivity tests.

2) About the generation cost function. Although we employ linear generation cost functions in objective function (1a) for the ease of discussion, the method remains intact if convex quadratic cost functions are taken into account, because quadratic terms in the Lagrangian function L will become linear after differentiation, and condition $\partial L/\partial p_i = 0$ in the KKT conditions gives rise to linear equations.

3) Sometimes, it is helpful to include complementarity constraint (4) in the form of (9) into MILP (12), because they constitute valid inequalities and tighten the lower bound in the branch-and-bound procedure. However, this strategy is not always useful, as it also complicates the feasible region.

4. Case studies

We conduct numeric tests on a modified IEEE 118-bus system.

Fig. 4. Five types DR functions [45].

Table 2
Computation Times With Different Load Responses (in seconds).

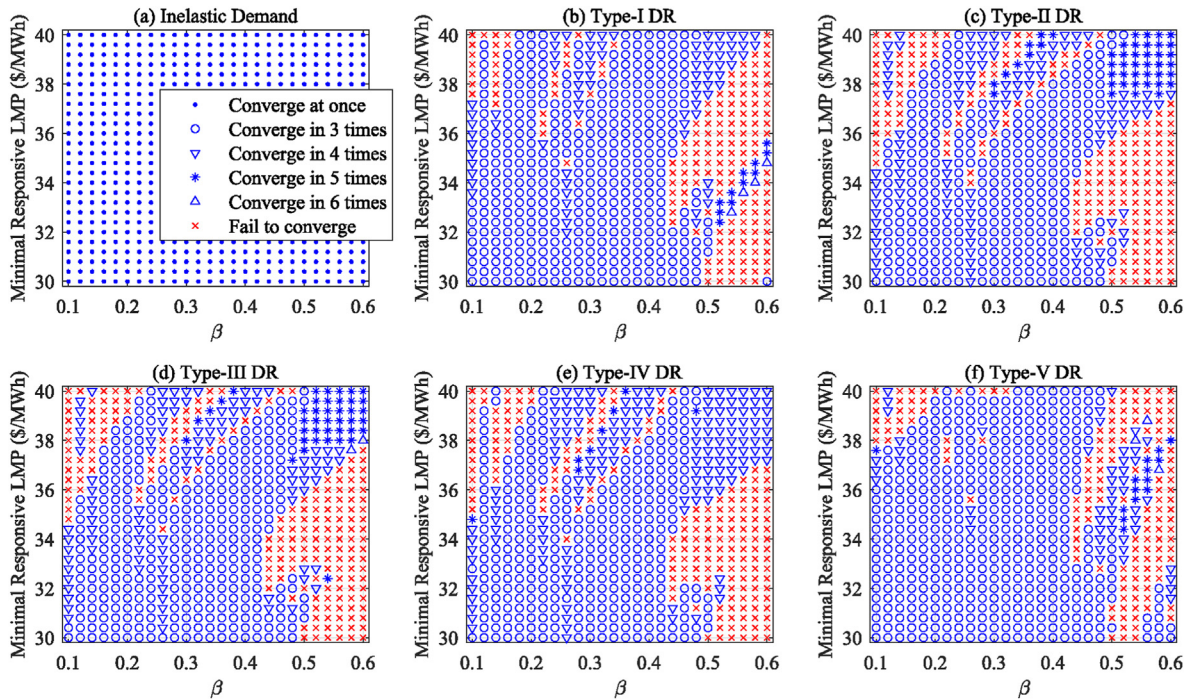| DR Type	Algorithm	DR participation level β					
		0.1	0.2	0.3	0.4	0.5	0.6
Inelastic	LP			0.019			
Type-I	MILP (12)	5.54	4.61	7.19	11.8	19.3	42.2
	Alg-FP	0.062(4)	0.052(3)	0.051(3)	0.055(3)	fail	fail
Type-II	MILP (12)	6.27	7.81	12.5	17.8	15.9	63.9
	Alg-FP	fail	0.049(3)	fail	0.060(3)	0.068(4)	fail
Type-III	MILP (12)	3.30	4.56	12.7	7.30	16.8	48.6
	Alg-FP	fail	0.053(3)	0.051(3)	0.051(3)	0.065(4)	fail
Type-IV	MILP (12)	4.42	4.03	10.8	18.5	26.6	48.0
	Alg-FP	fail	0.049(3)	fail	0.053(3)	0.065(4)	fail
Type-V	MILP (12)	3.68	1.58	5.62	5.58	14.0	20.0
	Alg-FP	0.048(3)	0.047(3)	0.047(3)	0.051(3)	0.061(4)	fail
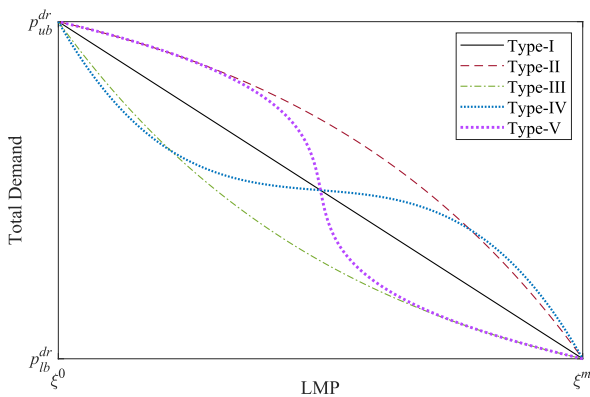
Fig. 5. Convergence test with different values of β and ξ^0.
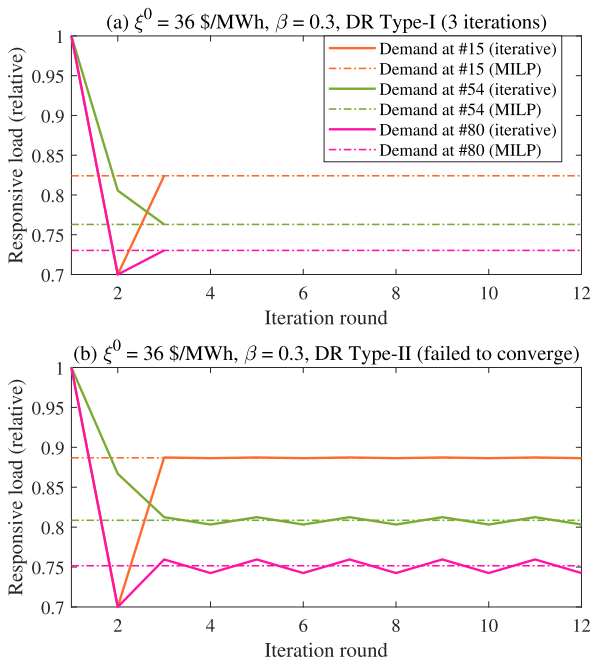
Fig. 6. Values of responsive load when performing DR program.

Table 3
System performances with different load types.

	Inelastic	Type-I	Type-IV	Type-V
Total demand (GW)	3.941	3.765	3.778	3.755
Total operation cost rate ($\times 10^3$ \$/h)	153.3	142.0	142.7	141.5
Cost rate saved by DR	–	7.32%	6.86%	7.65%
Average LMP (\$/MWh)	63.92	51.94	52.26	51.94
No. congested lines	6	4	4	3

suggested in Ref. [45], which are shown in Fig. 4. According to Ref. [45], these curves can reflect different sensitivities of responsive loads in different price intervals. We assume elastic loads take part in the DR program if LMP is in the interval $[\xi^0, \xi^0 + 20]$ \$/MWh; outside this interval, their demands are either maximum or minimum and do not vary with respect to LMP. We fix the maximum value p_{ub}^{dr} of elastic demands, and change the minimum value p_{lb}^{dr}; $\beta = p_{lb}^{dr}/p_{ub}^{dr}$ is called the DR participation level. By changing the values of ξ^0 and β, we investigate the system impact of DR loads and performances of the proposed method.

4.1. Computational efficiency

First, we test solver times of MILP (12) and Alg-FP with different DR functions and participation levels. For the inelastic cases, we directly solve DCOPF problem (1) and retrieve the dual variables associated with LMP. The solver time is less than a second since DCOPF is a linear program (LP). For the remaining cases, we solve DR program (1) via MILP (12) and using Alg-FP. Results are summarized in Table 2.

When β grows larger, a higher fraction of loads joins in the DR program, and the generation and demand get more interactive. Longer computation time is observed when solving MILP (12). By-and-large, the time grows with the increase in participation level β.
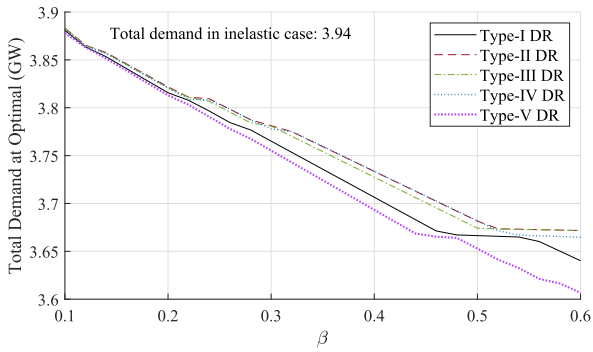
Complete system data can be found in Ref. [52]. Elastic demands connect to the system at buses #15 in area 1, #42, #49, #54, #56, #59, #60 in area 2, and #62, #80, #90 in area 3, accounting for about 20% of the total demand. Simulations are implemented on a laptop with Intel i5-8300H CPU and 16 GB memory. MILP is solved by CPLEX 12.8.

In practice, DR function is bid by consumers or calibrated from historical energy consumption data. We consider five DR functions

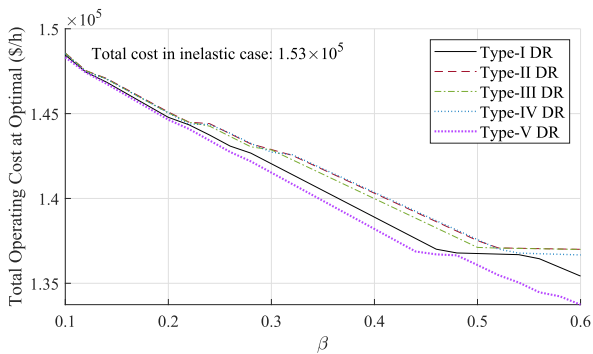**Fig. 7.** Total load demand with different DR types and participation levels.

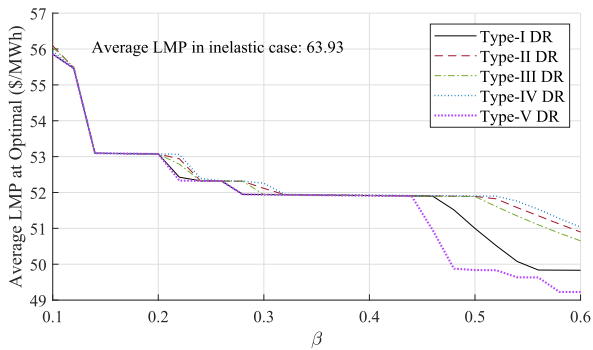**Fig. 8.** Total operating cost rate with different DR types and participation levels.

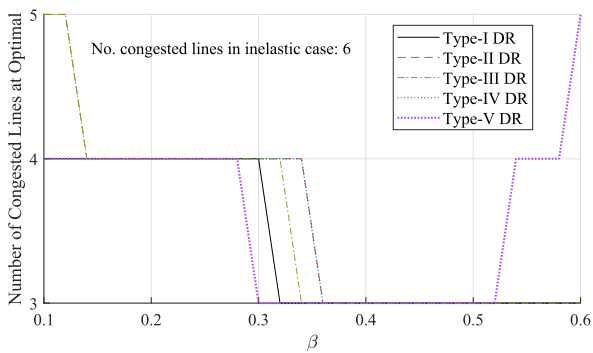**Fig. 9.** Average LMP with different DR types and participation levels.

Fig. 10. Congestion performance with different DR types and participation levels.

Nevertheless, the computation time of the proposed MILP model varies from several second to 1 min, which is efficient enough for practical use. Alg-FP is always faster because it only solves several LPs. When the DR participation level β changes from 0.1 to 0.6, Alg-FP fails to converge in 30% ~ 50% of the total six instances.

4.2. Convergence performance

As analyzed in Section 2, the equilibrium solution may not exist if the traditional LMP scheme is adopted. To show this effect, we solve problem (1) using Alg-FP and via MILP (12). If oscillation occurs in Alg-FP, there is no equilibrium solution for problem (1) under traditional LMP. Five DR functions with different values of ξ^0 and β are tested, and results are given in Fig. 5. Each subplot manifests one DR type, and each point corresponds to a pair of parameters (ξ^0, β). The red points manifest that Alg-FP fails to converge; the blue ones indicate the number of iterations before Alg-FP converges.

For the inelastic demand, no iteration is needed. For the five types of DR functions, there are approximately 20% ~ 30% cases in which Alg-FP fails to converge, implying that under the traditional LMP, market instability may not be a rare event and could happen no matter β is low or high; no regular pattern is found for such phenomenon. MILP (12) always has a solution which can be found in less than 2 min, because the value of LMP is softened at discontinuous points.

To better visualize the process and results of iteration, we pick two particular system configurations with $\xi^0 = 36$ \$/MWh and $\beta = 0.3$, in which Type-I and Type-II DR are adopted respectively. The change of three typical elastic demand (one in each area) are plotted in Fig. 6(a−b) with MILP equilibrium marked in dashed lines, where load is expressed by the proportion of its maximum power consumption. Under Type-I DR, Alg-FP takes three iterations to reach the equilibrium, and solving MILP gives the same results. Under Type-II DR, the responsive load takes two different groups of values repetitively in the iteration process, and Alg-FP fails to produce a traditional equilibrium. While the MILP model still gives a meaningful market-clearing point, accounting for the discontinuity of traditional LMP scheme.

4.3. Impact on system performances

We investigate the impact of DR on system performances from four aspects. Three types of DR functions are examined, including the linear case (Type-I) and two extreme cases (Type-IV, Type-V). $\xi^0 = 36$ \$/MWh and $\beta = 0.3$ are used in our tests. Results are exhibited in Table 3, where

$$\text{Average LMP} = \frac{\xi^{\mathrm{T}} P_D}{\mathbf{1}^{\mathrm{T}} P_D} \tag{13}$$

By introducing responsive demands, a certain fraction of the total demand switches to respond to the electricity price, leading to the reduction of the total cost, the average LMP, and the number of congested lines at the equilibrium solution. A higher cost saving is observed with Type-V DR function in which load is more sensitive when the price is either high or low, motivating more significant decrease in demand.

For further analysis of the influence brought by increasing participation of DR loads, similar tests are conducted by changing β from 0.1 to 0.6, while ξ^0 remains the same. Results are plotted in Figs. 7−10. Apparently, for all DR types, the total demand and operation cost decrease with the growth of β. Nevertheless, when $\beta \leq 0.2$, the impacts of different DR functions show little difference. The influence on demand and cost reduction becomes more

evident for $\beta \geq 0.3$, and system average LMP for $\beta \geq 0.45$. It is also observed that if the percentage of Type V DR is high, the number of congested lines is not monotonic: 5 lines are congested when $\beta = 0.6$, which is even more than the case with $\beta = 0.1$. In spite of the fact that more line flow constraints are binding, the total cost and the average LMP still exhibit a decreasing trend. This phenomenon largely depends on system data.

5. Conclusions

This paper discusses the economic dispatch problem with LMP-dependent demands. The difficulty caused by the traditional LMP scheme is revealed, and the LMP concept at discontinuous points is revamped to guarantee the existence of an equilibrium solution. An MILP model is proposed to solve the interactive dispatch problem. Numeric experiments on a 118-bus system validate the computational efficiency and effectiveness of the proposed model.

Under traditional LMP scheme, the non-existence of an equilibrium solution may lead to market instability (interpreted by oscillation in numeric tests) with non-negligible possibility. The proposed DR program with redefined LMP concept can reflect the effect of DR integration including: 1) Transmission congestion can be alleviated via the DR program, where load peak and market-clearing price are reduced monotonically with the increasing DR participation level; 2) The system impact of different DR functions can hardly be distinguished unless the DR participation level is sufficiently high (not smaller than 5% of the total demand in our case), and the linear DR function has moderate performance over the entire price range.

In conclusion, the method in this paper provides a non-iterative approach to retrieving practical market-clearing strategy under DCOPF with LMP-dependent demands. The market equilibrium condition consists of the KKT condition of DCOPF and the linearized demand function. It can be embedded in more sophisticated optimization problems that study the strategic behavior or market power of generation companies in the market environment. In such problems, the market-clearing problem is usually formulated as constraint sets in order to be jointly solved together with the decision-making problem of strategic participants.

Declaration of competing interest

The authors declare that they have no known competing financial interests or personal relationships that could have appeared to influence the work reported in this paper.

Credit author statement

Ziqi Shen: Software, Validation, Writing − original draft, Wei Wei: Conceptualization, Methodology, Formal analysis, Writing − original draft, Lei Wu: Conceptualization, Formal analysis, Writing − review & editing, Miadreza Shafie-khah: Writing − review & editing, João P. S. Catalão: Conceptualization, Writing − review & editing

Appendix A. Error Bound of Linear Interpolation

We now prove that the error bound of linear interpolation satisfies (8). Suppose the demand function $P^R_{D_j}(\xi_j)$ is second-order continuously differentiable on interval $[\xi^{(1)}, \xi^{(2)}]$. Assume the linear interpolation error of $P^R_{D_j}(\xi_j)$ on interval $[\xi^{(1)}, \xi^{(2)}]$ has the form

$$R_{1j}(\xi_j) = P^R_{D_j}(\xi_j) - P_{1j}(\xi_j) = K(\xi_j)(\xi_j - \xi^{(1)})(\xi_j - \xi^{(2)})$$

where $K(\xi_j)$ is an undetermined function of ξ_j, as the linear interpolation at the endpoints must satisfy

$$R_{1j}(\xi^{(i)}) = P^R_{D_j}(\xi^{(i)}) - P_{1j}(\xi^{(i)}) = 0, i = 1, 2$$

Introduce auxiliary function of t

$$\phi(t) = P^R_{D_j}(t) - P_{1j}(t) - K(\xi_j)(t - \xi^{(1)})(t - \xi^{(2)})$$

We have $\phi(\xi_j) = 0$ and $\phi(\xi^{(i)}) = R_{1j}(\xi^{(i)}) = 0$, $i = 1, 2$. Therefore, $\phi(t)$ has at least three zero points on interval $[\xi^{(1)}, \xi^{(2)}]$. Using Rolle's Theorem for twice, we can derive that

$$\left. \frac{\partial^2 \phi(t)}{\partial t^2} \right|_{t=c_\xi} = \left. \frac{\partial^2}{\partial t^2}\left(P^R_{D_j}(t) - P_{1j}(t) - K(\xi_j)\left(t - \xi^{(1)}\right)\left(t - \xi^{(2)}\right)\right) \right|_{t=c_\xi}$$

$$= \frac{d^2}{d\xi_j^2} P^R_{D_j}(c_\xi) - 2K(\xi_j) = 0$$

for some $c_\xi \in [\xi, \xi + h]$. The interpolation error is thus

$$R_{1j}(\xi_j) = P^R_{D_j}(\xi_j) - P_{1j}(\xi_j) = \frac{(\xi_j - \xi^{(1)})(\xi_j - \xi^{(2)})}{2} \frac{d^2}{d\xi_j^2} P^R_{D_j}(c_\xi)$$

where c_ξ depends on ξ_j. Letting $[\xi^{(1)}, \xi^{(2)}] = [\xi, \xi + h]$, the error bound satisfies

$$P^R_{D_j}(\xi_j) - P_{1j}(\xi_j) \quad \leq max_{\xi_j \in [\xi, \xi+h]}\left\{\frac{d^2}{d\xi_j^2} P^R_{D_j}(c_\xi)\frac{(\xi_j - \xi)(\xi + h - \xi_j)}{2}\right\}$$

$$\leq D_M max_{\xi_j \in [\xi, \xi+h]}\left\{\frac{(\xi_j - \xi)(\xi + h - \xi_j)}{2}\right\}$$

$$\leq \frac{D_M h^2}{8} = O\left(h^2\right)$$

which proves (8).

References

[1] Paterakis N, Erdinç O, Catalão JPS. An overview of demand response: Key-elements and international experience. Renew Sustain Energy Rev 2017;69: 871−91.
[2] Dranka G, Ferreira P. Review and assessment of the different categories of demand response potentials. Energy 2019;179:280−94.
[3] Wang F, Xu H, Xu T, Li K, Shafie-khah M, Catalão JPS. The values of market-based demand response on improving power system reliability under extreme circumstances. Appl Energy 2017;193:220−31.
[4] Fell MJ, Shipworth D, Huebner G, Elwell C. Public acceptability of domestic demand-side response in great britain: the role of automation and direct load control. Energy Res Soc Sci 2015;9:72−84.
[5] Assessment of demand response and advanced metering federal energy regulatory commission, Tech Rep.
[6] Ghasemi A, Mortazavi SS, Mashhour E. Integration of nodal hourly pricing in day-ahead sdc (smart distribution company) optimization framework to effectively activate demand response. Energy 2015;86:649−60.
[7] Paterakis NG, Erdinç O, Bakirtzis AG, Catalão JPS. Optimal household appliances scheduling under day-ahead pricing and load-shaping demand response strategies. IEEE Trans Ind Inform 2015;11(6):1509−19.
[8] Parvania M, Fotuhi-Firuzabad M. Demand response scheduling by stochastic SCUC. IEEE Trans Smart Grid 2010;1(1):89−98.
[9] Nikzad M, Mozafari B, Bashirvand M, Solaymani S, Ranjbar AM. Designing time-of-use program based on stochastic security constrained unit commitment considering reliability index. Energy 2012;41(1):541−8.
[10] Zhao L, Zeng B. Robust unit commitment problem with demand response and

wind energy. In: Proc. IEEE power engineering society general meeting, san Diego, CA, USA; 2012. p. 1–8.

[11] Zhao C, Wang JWJ, Guan Y. Multi-stage robust unit commitment considering wind and demand response uncertainties. IEEE Trans Power Syst 2013;28(3): 2708–17.

[12] do Prado J, Qiao W. A stochastic decision-making model for an electricity retailer with intermittent renewable energy and short-term demand response. IEEE Trans Smart Grid 2019;10(3):2581–92.

[13] Ferreira R, Barroso MCL. Demand response models with correlated price data: a robust optimization approach. Appl Energy 2012;96:133–49.

[14] Chen Z, Wu L, Fu Y. Real-time price-based demand response management for residential appliances via stochastic optimization and robust optimization. IEEE Trans Smart Grid 2012;3(4):1822–31.

[15] Vahid-Ghavidel M, Mahmoudi N, Mohammadi-Ivatloo B. Self-scheduling of demand response aggregators in short-term markets based on information gap decision theory. IEEE Trans Smart Grid 2019;10(2):2115–26.

[16] Liu G, Xu Y, Tomsovic K. Bidding strategy for microgrid in day-ahead market based on hybrid stochastic/robust optimization. IEEE Trans Smart Grid 2016;7(1):227–37.

[17] Sheikhi A, Bahrami S, Ranjbar AM. An autonomous demand response program for electricity and natural gas networks in smart energy hubs. Energy 2015;89:490–9.

[18] Cui H, Li F, Hu Q, Bai L, Fang X. Day-ahead coordinated operation of utility-scale electricity and natural gas networks considering demand response based virtual power plants. Appl Energy 2016;176:183–95.

[19] Wang J, Zhong H, Ma Z, Xia Q, Kang C. Review and prospect of integrated demand response in the multi-energy system. Appl Energy 2017;202:772–82.

[20] Alipour M, Zare K, Seyedi H, Jalali M. Real-time price-based demand response model for combined heat and power systems. Energy 2019;168:1119–27.

[21] Tian M-W, Talebizadehsardari P. Energy cost and efficiency analysis of building resilience against power outage by shared parking station for electric vehicles and demand response program. Energy 2021;215:119058.

[22] He C, Zhang X, Liu T, Wu L. Distributionally robust scheduling of integrated gas-electricity systems with demand response. IEEE Trans Power Syst 2019;34(5):3791–803.

[23] Bai L, Li F, Cui H, Jiang T, Sun H, Zhu J. Interval optimization based operating strategy for gas-electricity integrated energy systems considering demand response and wind uncertainty. Appl Energy 2016;167:270–9.

[24] Chen Z, Zhang Y, Tang W, Lin X, Li Q. Generic modelling and optimal day-ahead dispatch of micro-energy system considering the price-based integrated demand response. Energy 2019;176:171–83.

[25] Tabar VS, Ghassemzadeh S, Tohidi S. Energy management in hybrid microgrid with considering multiple power market and real time demand response. Energy 2019;174:10–23.

[26] Shahryari E, Shayeghi H, Mohammadi-ivatloo B, Moradzadeh M. An improved incentive-based demand response program in day-ahead and intra-day electricity markets. Energy 2018;155:205–14.

[27] Shahryari E, Shayeghi H, Mohammadi-ivatloo B, Moradzadeh M. A copula-based method to consider uncertainties for multi-objective energy management of microgrid in presence of demand response. Energy 2019;175: 879–90.

[28] Hlalele TG, Zhang J, Naidoo RM, Bansal RC. Multi-objective economic dispatch with residential demand response programme under renewable obligation. Energy 2021;218:119473.

[29] Zugno M, Morales JM, Pinson P, Madsen H. A bilevel model for electricity retailers' participation in a demand response market environment. Energy Econ 2013;36:182–97.

[30] Wei W, Liu F, Mei S. Energy pricing and dispatch for smart grid retailers under demand response and market price uncertainty. IEEE Trans Smart Grid 2015;6(3):1364–74.

[31] Zhang C, Wang Q, Wang J, Pinson P, Morales JM, Østergaard J. Real-time procurement strategies of a proactive distribution company with aggregator-based demand response. IEEE Trans Smart Grid 2018;9(2):766–76.

[32] Nizami MSH, Hossain MJ, Amin BMR, Fernandez E. A residential energy management system with bi-level optimization-based bidding strategy for day-ahead bi-directional electricity trading. Appl Energy 2020;261:114322.

[33] Dadashi M, Haghifam S, Zare K, Haghifam M-R, Abapour M. Short-term scheduling of electricity retailers in the presence of demand response aggregators: a two-stage stochastic bi-level programming approach. Energy 2020;205:117926.

[34] Liu N, He L, Yu X, Ma L. Multiparty energy management for grid-connected microgrids with heat- and electricity-coupled demand response. IEEE Trans Ind Inform 2018;14(5):1887–97.

[35] Li P, Wang Z, Wang J, Yang W, Guo T, Yin Y. Two-stage optimal operation of integrated energy system considering multiple uncertainties and integrated demand response. Energy 2021;225:120256.

[36] Zheng S, Sun Y, Li B, Qi B, Shi K, Li Y, Tu X. Incentive-based integrated demand response for multiple energy carriers considering behavioral coupling effect of consumers. IEEE Trans Smart Grid 2020;11(4):3231–45.

[37] Monfared HJ, Ghasemi A, Loni A, Marzband M. A hybrid price-based demand response program for the residential micro-grid. Energy 2019;185:274–85.

[38] Li N, Chen L, Dahleh MA. Demand response using linear supply function bidding. IEEE Trans Smart Grid 2015;6(4):1827–38.

[39] Eksin C, Delic H, Ribeiro A. Demand response management in smart grids with heterogeneous consumer preferences. IEEE Trans Smart Grid 2015;6(6): 3082–94.

[40] Belhaiza S, Baroudi U, Elhallaoui I. A nash-stackelberg game approach in regional energy market considering users' integrated demand response. Energy 2019;175:456–70.

[41] Belhaiza S, Baroudi U, Elhallaoui I. A game theoretic model for the multi-periodic smart grid demand response problem. IEEE Syst J 2020;14(1): 1147–58.

[42] Wang K, Ouyang Z, Krishnan R, Shu L, He L. A game theory-based energy management system using price elasticity for smart grids. IEEE Trans Ind Inform 2015;11(6):1607–16.

[43] Yang J, Guo W, Ma K, Tian Z, Dou C. Strategic equilibrium of economic dispatch in smart grid with a bi-level game approach. IET Gener Transm Distrib 2020;14(2):2227–36.

[44] Chai B, Chen J, Yang Z, Zhang Y. Demand response management with multiple utility companies: a two-level game approach. IEEE Trans Smart Grid 2014;5(2):722–31.

[45] Zhao Z, Wu L, Song G. Convergence of volatile power markets with price-based demand response. IEEE Trans Power Syst 2014;29(5):2107–18.

[46] Wei W, Wang J, Wu L. Distribution optimal power flow with real-time price elasticity. IEEE Trans Power Syst 2018;33(1):1097–8.

[47] Fu Y, Li Z. Different models and properties on LMP calculations. In: Proc. IEEE power engineering society general meeting. Montreal, Que.: Canada; 2006. p. 1–11.

[48] Li F. Continuous locational marginal pricing (CLMP). IEEE Trans Power Syst 2007;22(4):1638–46.

[49] Fletcher R, Leyffer S, Ralph D, Scholtes S. Local convergence of SQP methods for mathematical programs with equilibrium constraints. SIAM J Optim 2006;17(1):259–86.

[50] Vielma JP, Nemhauser GL. Modeling disjunctive constraints with a logarithmic number of binary variables and constraints. Math Program 2011;128(1–2): 49–72.

[51] Fortuny-Amat J, Mccarl B. A representation and economic interpretation of a two-level programming problem. J Oper Res Soc 1981;32(9):783–92.

[52] (2020). [link]. URL https://sites.google.com/view/springshenworkbench.